

JOURNAL OF GLACIOLOGY



CAMBRIDGE
UNIVERSITY PRESS

THIS MANUSCRIPT HAS BEEN SUBMITTED TO THE JOURNAL OF GLACIOLOGY AND HAS NOT BEEN PEER-REVIEWED.

Sub-kilometre scale distribution of snow depth on Arctic sea ice from Soviet drifting stations

Journal:	<i>Journal of Glaciology</i>
Manuscript ID	Draft
Manuscript Type:	Article
Date Submitted by the Author:	n/a
Complete List of Authors:	Mallett, Robbie; University College London, Earth Sciences Stroeve, Julianne; University of Manitoba, (2) Centre for Earth Observation Science (CEOS); University College London, Earth Sciences; National Snow and Ice Data Center Tsamados, Michel; University College London, Earth Sciences Willatt, Rosemary; University College London, Earth Sciences Newman, Thomas; University College London, Earth Sciences Nandan, Vishnu; University of Manitoba, (2) Centre for Earth Observation Science (CEOS) Landy, Jack; UiT The Arctic University of Norway Itkin, Polona; UiT The Arctic University of Norway; Colorado State University, Cooperative Institute for Research in the Atmosphere Oggier, Marc; International Arctic Research Center, Jaggi, Matthias; WSL Institute for Snow and Avalanche Research SLF, Snow and Permafrost Perovich, Donald; Dartmouth College, Thayer School of Engineering
Keywords:	Sea ice, Snow, Wind-blown snow

Abstract:	<p>The sub-kilometre scale distribution of snow depth on Arctic sea ice impacts atmosphere-ice fluxes of heat and light, and is of importance for satellite estimates of sea ice thickness from both radar and lidar altimeters. While information about the mean of this distribution is increasingly available from modelling and remote sensing, the full distribution cannot yet be resolved. We analyse 33539 snow depth measurements from 499 transects taken at Soviet drifting stations between 1955 and 1991 and derive a simple statistical distribution for snow depth over multi-year ice as a function of only the mean snow depth. We then evaluate this snow depth distribution against snow depth transects that span first-year ice to multiyear ice from the MOSAiC, SHEBA and AMSR-Ice field campaigns. Because the distribution can be generated using only the mean snow depth, it can be used in the downscaling of several existing snow depth products for use in flux modelling and altimetry studies.</p>

SCHOLARONE™
Manuscripts

Sub-kilometre scale distribution of snow depth on Arctic sea ice from Soviet drifting stations

Robbie D.C. MALLETT,¹ Julienne C. STROEVE,^{1,2,3} Michel TSAMADOS,¹ Rosemary WILLATT,¹ Thomas NEWMAN,¹ Vishnu NANDAN,³ Jack C. LANDY,⁴ Polona ITKIN,^{4,5} Marc OGGIER,⁶ Matthias JAGGI⁷ and Don PEROVICH⁸

¹*Centre for Polar Observation and Modelling, UCL, London, UK*

²*National Snow and Ice Data Center, University of Colorado, Boulder, CO, USA*

³*Centre for Earth Observation Science, University of Manitoba, Winnipeg, Canada*

⁴*Department of Physics and Technology, UiT The Arctic University of Norway, Tromsø, Norway*

⁵*Cooperative Institute for Research in the Atmosphere,*

Colorado State University, Fort Collins, CO, USA

⁶*Geophysical Institute, University of Alaska Fairbanks, Fairbanks, AK, USA*

⁷*WSL Institute for Snow and Avalanche Research SLF, Davos Dorf, Switzerland*

⁸*Thayer School of Engineering, Dartmouth College, Hanover, NH, USA*

Correspondence: Robbie Mallett <robbie.mallett.17@ucl.ac.uk>

ABSTRACT.

The sub-kilometre scale distribution of snow depth on Arctic sea ice impacts atmosphere-ice fluxes of heat and light, and is of importance for satellite estimates of sea ice thickness from both radar and lidar altimeters. While information about the mean of this distribution is increasingly available from modelling and remote sensing, the full distribution cannot yet be resolved. We analyse 33539 snow depth measurements from 499 transects taken at Soviet drifting stations between 1955 and 1991 and derive a simple statistical distribution for snow depth over multi-year ice as a function of only the mean snow depth. We then evaluate this snow depth distribution against snow depth transects that span first-year ice to multiyear ice from the MOSAiC, SHEBA and AMSR-Ice field campaigns. Because the distribution can be generated

28 using only the mean snow depth, it can be used in the downscaling of several
29 existing snow depth products for use in flux modelling and altimetry studies.

30 INTRODUCTION

31 The snow cover of Arctic sea ice insulates the underlying ice from solar radiation in the summer and cold
32 temperatures in the winter. In addition, snow impacts the propagation of laser and radar pulses from
33 satellite altimeters, affecting the timing of their return. This importance has driven the development of a
34 range of modelling and remote sensing approaches to accurately characterise the snow cover (see Zhou and
35 others, 2021, for intercomparison of several products). Satellite remote sensing approaches (e.g. Rostosky
36 and others, 2018; Lawrence and others, 2018) are generally limited by their low (multi-kilometre) spatial
37 resolution, which has the effect of averaging out kilometre and sub-kilometre scale variability. Modelling
38 approaches (e.g. Petty and others, 2018; Liston and others, 2020; Stroeve and others, 2020a) have similar
39 limitations, with grid resolutions not falling below tens of kilometres. This in part reflects the coarse spatial
40 resolution of standard atmospheric reanalysis and sea ice drift products.

41 This lower-bound on spatial resolution is a significant barrier to scientific progress, as the effects of
42 snow on fluxes and sea ice thickness retrievals cannot be characterised solely by the mean snow depth
43 in a grid-cell of a traditional data product (Iacozza and Barber, 1999), so a *sub-grid* scale snow depth
44 distribution must be employed (e.g. Petty and others, 2020; Glissenaar and others, 2021). For instance,
45 the amount of light incident on the ice surface in a multi-kilometre grid cell is sensitive to the fractional
46 coverage of snow which is *optically thin* ($< \sim 15$ cm for dry snow; Warren, 2019). This area cannot be
47 straightforwardly gleaned from modelling or satellite observations of the mean snow depth in the grid cell
48 (Stroeve and others, 2021).

49 In the example above, the area of optically thin snow within a larger area of level ice with given mean
50 thickness will be primarily dictated by wind redistribution (Moon and others, 2019). Snow is dynamically
51 transported through wind suspension and saltation, and is eroded and deposited heterogeneously around ice
52 topography such as ridges and hummocks (Sturm and others, 2002; Chung and others, 2011). Furthermore,
53 turbulence-induced features such as sastrugi introduce depth variability even on level ice (Eicken and others,
54 1994; Massom and others, 1997). The probability of snow transport and redistribution is dependent on
55 its bulk and microstructural properties such as density and bond-radius (Filhol and Sturm, 2015). The

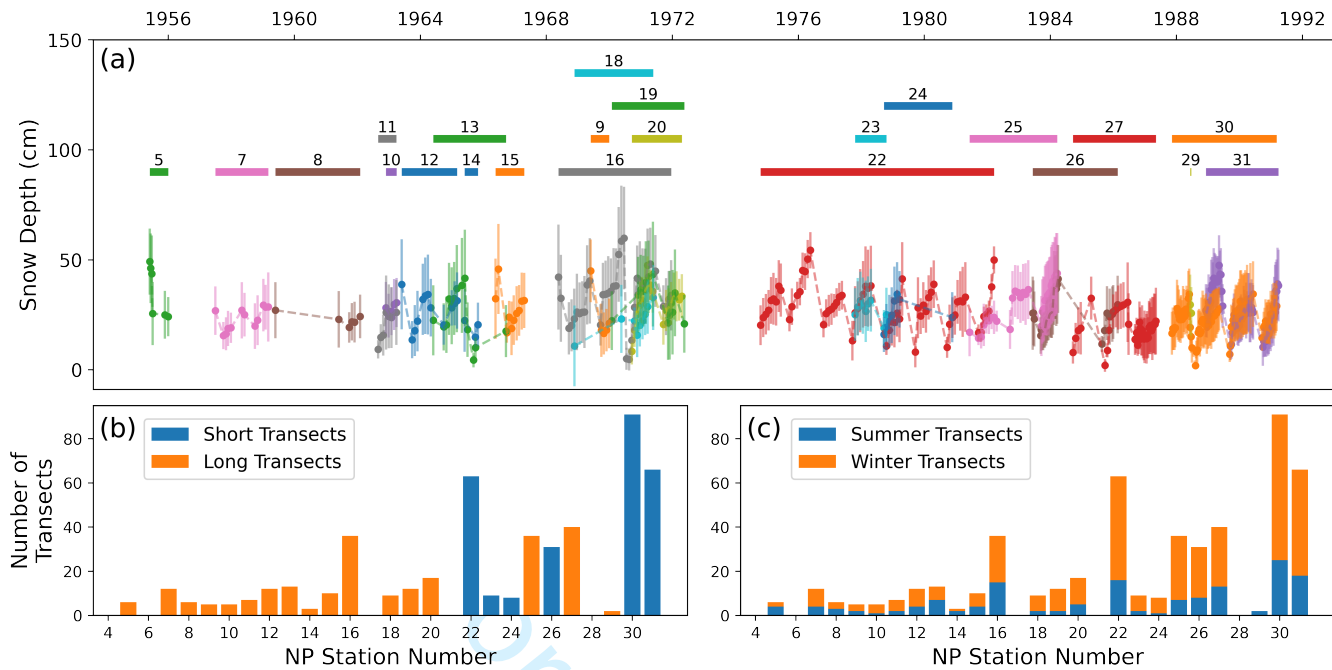


Fig. 1. (a) Operational periods of the NP stations contributing in this study. Bars at top indicate the time period between the first and last snow depth transect of the station. Solid circles indicate mean snow depth of transects, with vertical bars indicating one standard deviation in snow depth (b) The number of transects measured by each station, broken down by transect length (500m vs. 1000m). (c) Number of transects measured by each station broken down by summer (May-Sep) and winter (Oct-Apr).

56 combination of these factors makes deterministic modelling of snow redistribution a major challenge when
 57 the local ice topography is not known to a high level of detail (e.g. Liston and others, 2018), which is
 58 generally the case on sea ice. In this paper we derive a statistical model for the snow depth distribution
 59 based on the large number of snow depth measurements taken at Soviet drifting stations.

60 Snow transects from Soviet drifting stations

61 We analyse the results of snow depth transects performed at Soviet North Pole (NP) drifting stations
 62 between 1955 and 1991. These were crewed stations that drifted year-round in the Arctic Ocean while
 63 measuring a range of atmospheric, oceanographic and cryospheric parameters on what was generally multi-
 64 year sea ice. In particular we examine 33539 snow depth measurements from 499 transects from NP stations
 65 5 - 31. Snow transects did not begin until NP 5, and the NP program was halted in 1991. While it was
 66 restarted in 2003, these data are not publicly available.

67 Snow depths were measured every 10 m along a line of either 500 or 1000 m long when snow depth was

Mallett and others:

at least 5 cm and more than 50% of the surrounding area was snow covered. 166 transects were 500 m long and 333 were around 1000 m long, with transects prior to 1974 generally being of the 500 m type. The direction of the line was chosen randomly but did deviate where hummocks were present, and was at least 500 m from the station at its closest point. We note that this deviation around hummocks may introduce a bias in the snow depth measurements to sample more level ice with thinner snow. Where successive transects were taken at the same station, each was offset by 3 m from the previous line.

RESULTS

We now present a method for transforming an estimate of mean snow depth (from remote sensing or modelling) into a distribution of snow depths. We first characterise the linear relationship between the standard deviation of snow depths measured along a transect and the mean of that transect (Fig. 2a). When a linear regression is performed (and forced through the origin), the root-mean-square of the residuals is 3.20 cm, meaning that the standard deviation of the transect depths can be predicted with this standard-error where the mean is known. For every 10 cm increase in the mean snow depth, we find the standard deviation of the snow depths to increase by 4.17 cm.

$$\sigma_D = 0.417 \times \bar{D} \quad (1)$$

Where σ_D is the standard deviation of snow depth in a transect, and \bar{D} the mean depth of the transect. We then convert all NP station snow depth measurements into depth-anomalies from their respective transect means (by subtracting the transect-mean value from each). We further transform these anomalies (measured in centimetres) into relative anomalies from the mean by dividing them by the standard deviation of their respective transects. When the distribution of these relative anomalies from the mean are plotted and normalised, a probability distribution is formed (Fig. 2b). To this distribution we fit a skewed-normal curve.

Our skewed normal distribution function is defined following O'Hagan and Leonard (1976) and Azzalini and Capitanio (1999) such that:

$$f(\sigma_D) = \frac{2}{\omega} \phi \left(\frac{\sigma_D - \xi}{\omega} \right) \Phi \left(a \frac{\sigma_D - \xi}{\omega} \right) \quad (2)$$

where:

$$\phi(x) = \frac{1}{\sqrt{2\pi}} e^{-\frac{x^2}{2}} \quad \text{and} \quad \Phi(x) = \frac{1}{2} \left(1 + \operatorname{erf}\left(\frac{x}{\sqrt{2}}\right) \right) \quad (3)$$

92 with a being the skewness parameter, ξ being a location parameter, ω being a scaling parameter, and
 93 erf being the error function. We find the values of the three parameters to be $a = 2.54$, $\xi = -1.11$, $\omega = 1.50$.
 94 We also find that the skew-normal curve provides a marginally better fit to the data than a log-normal
 95 curve, reducing the root mean squared error by 8.5%.

96 We repeat this process for the winter and summer seasons individually (October-April, May-September).
 97 While the scaling of standard deviation with mean depth is slightly steeper in Summer (Fig. 2c), the shape
 98 of the summer probability distribution is not significantly different (Fig. 2d). This difference in the scaling
 99 is relatively small compared to the uncertainty and residuals in the regression, and as such we opt for a
 100 singular analysis, considering all transects from all months.

101 The above method allows the standard deviation of the snow depth to be estimated from the mean
 102 snow depth (Fig. 2a). When both of these quantities are known, the snow depth distribution may be
 103 calculated using the skewed normal curve shown in Fig. 2b.

104 For instance, if the mean snow depth is assumed to be 0.5 metres, then the standard deviation of the
 105 snow depth distribution is estimated using Eq. 1 such that $\sigma_D = 0.209 \pm 0.032$. Multiplying the x axis of
 106 Fig. 2b by this factor, it can be inferred (for example) that the probability of randomly sampled snow of
 107 less than 30 cm is 17%, the chance of sampling snow thicker than 1 metre deep is 1.8%.

108 For calculations of light flux through thin snow, it may be found that for snow of a mean thickness of
 109 0.5 m, the probability of snow being of less than 15 cm is around 2%. The same probability for snow of
 110 0.25 m is around 17%.

111 When applied in this way, the method described above functions as a statistical *model* for the snow
 112 depth distribution, and we use this term interchangeably with ‘method’ when evaluating its performance in
 113 the next section.

114 Negative Snow Depths

115 The use of a skewed normal distribution (or any normal distribution) results in a small fraction of negative
 116 snow depths. We find that the total fraction is relatively constant at 0.1% in the 0 - 50 cm range of mean
 117 snow depths. Above this range, it transitions to a linear decline with increasing mean snow depth, dropping
 118 below 0.075% for snow depths larger than 200 cm.

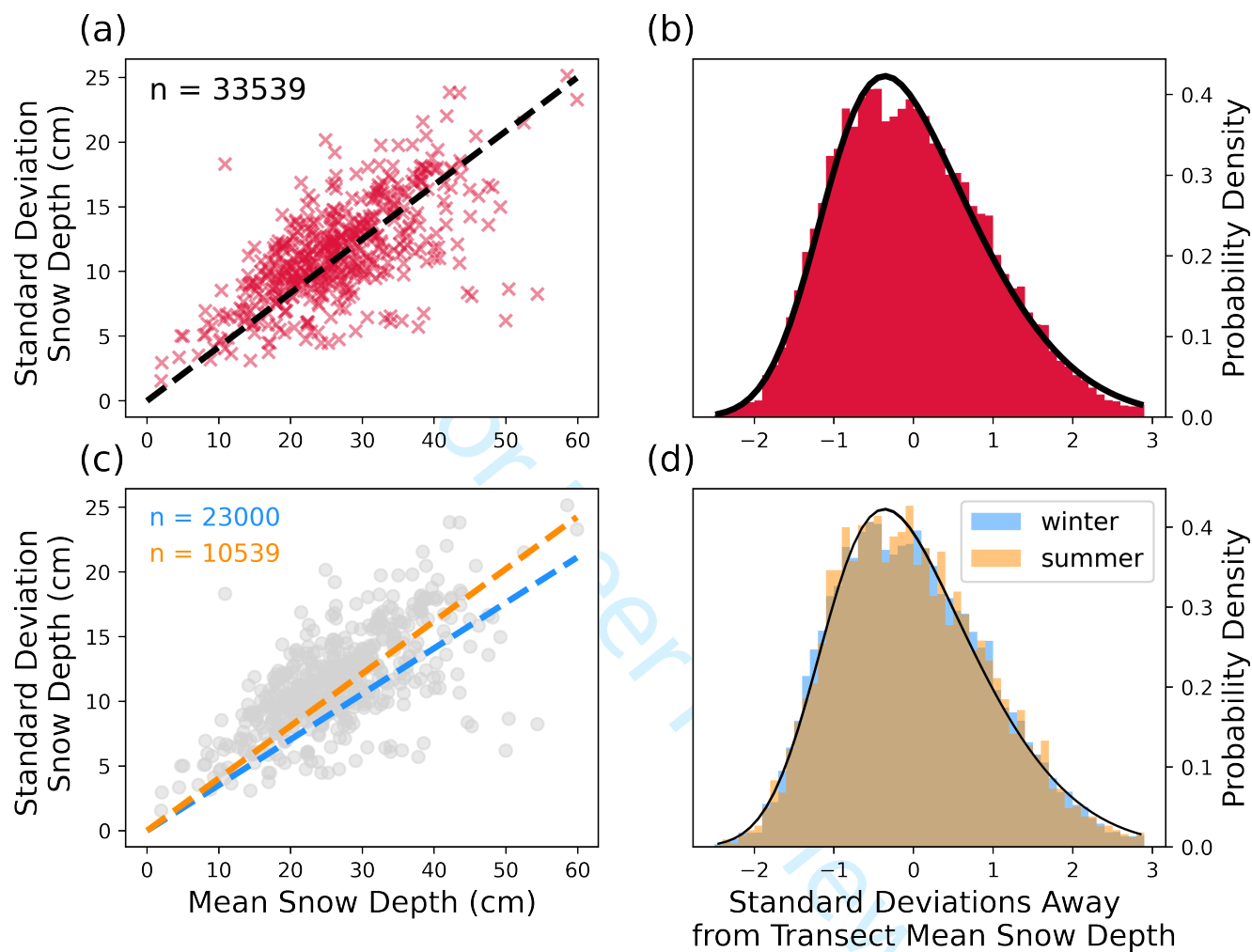


Fig. 2. (a) Relationship between a transect's mean snow depth and the standard deviation. The slope of the regression (forced through the origin) is 0.41, the root-mean-squared-residual is 3.20 cm, and the Pearson correlation coefficient (r value) is 0.66 (b) The probability density of a snow depth being measured such that it is a given number of standard deviations from the mean of the transect. The empirical distribution is given in red from drifting station data and a skewed-normal curve is fitted in black. (c) Same as a, but with individual regressions for winter and summer transects. (d) same as b, but with individual probability density distributions for winter and summer transects. The two seasonal skew-normal fits (black) are visually indistinguishable.

119 Because the fraction of negative snow depths does not exceed 0.1%, we treat it as negligible in the
120 analysis that follows. However, if this distribution were implemented in a snow-conserving model it would
121 be necessary to modify the low-tail of the distribution. This could be done by merging the distribution
122 with an exponential curve at low values, or by truncating it at zero and redistributing the coverage so
123 that the area under the probability distribution is unity. In the redistribution case, it would be possible
124 to either scale the whole curve by a small amount, or instead preferentially add the 'lost' coverage to the
125 low-end of the distribution. We stress however that the effect of this would be extremely small (and not
126 noticeable in the analysis of this paper), and so is only necessary for applications where snow must be
127 precisely conserved.

128 DISCUSSION

129 Cross-validation

130 We now evaluate the consistency of our snow depth distribution method with a leave-one-out-cross-
131 validation (LOOCV) approach (Stone, 1978). To do this we select a single transect and recalculate the
132 skewed-normal curve using the remaining 498 transects. We then assess the goodness-of-fit of the curve
133 against the selected transect. This is performed iteratively for each transect such that 499 goodness-of-fit
134 statistics are generated. We calculate the goodness-of-fit using the root-mean-square error (RMSE) for the
135 fitted probability distribution and that of the transect, using ten equal-width depth bins that span from 0
136 cm to the maximum depth measured.

137 This cross-validation exercise allows for the estimation of model skill as a function of different variables,
138 such as the transect's length, its mean depth and the month in which it was performed (Fig. 3a - c). We
139 also investigate whether the snow depth distribution of a transect can be better predicted with the model
140 presented here (the 'NP model') when its corresponding station has contributed many other transects to
141 the distribution (Fig. 3d).

142 We first show that the NP model's skill is very similar when applied to both long and short NP
143 transects (Fig. 3a). The mean RMSE for long and short transects is 0.053 and 0.057 cm respectively (a
144 difference of 7%). This similarity is to be expected, with the difference likely reflecting the more incomplete
145 sampling of the local snow depth distribution by a shorter transect. We also show that the skill of the NP
146 distribution is relatively independent of the depth of the transect. The skill of the method is maximal for
147 snow distributions with means in the range of 20 - 40 cm. Transects where the model exhibited lowest

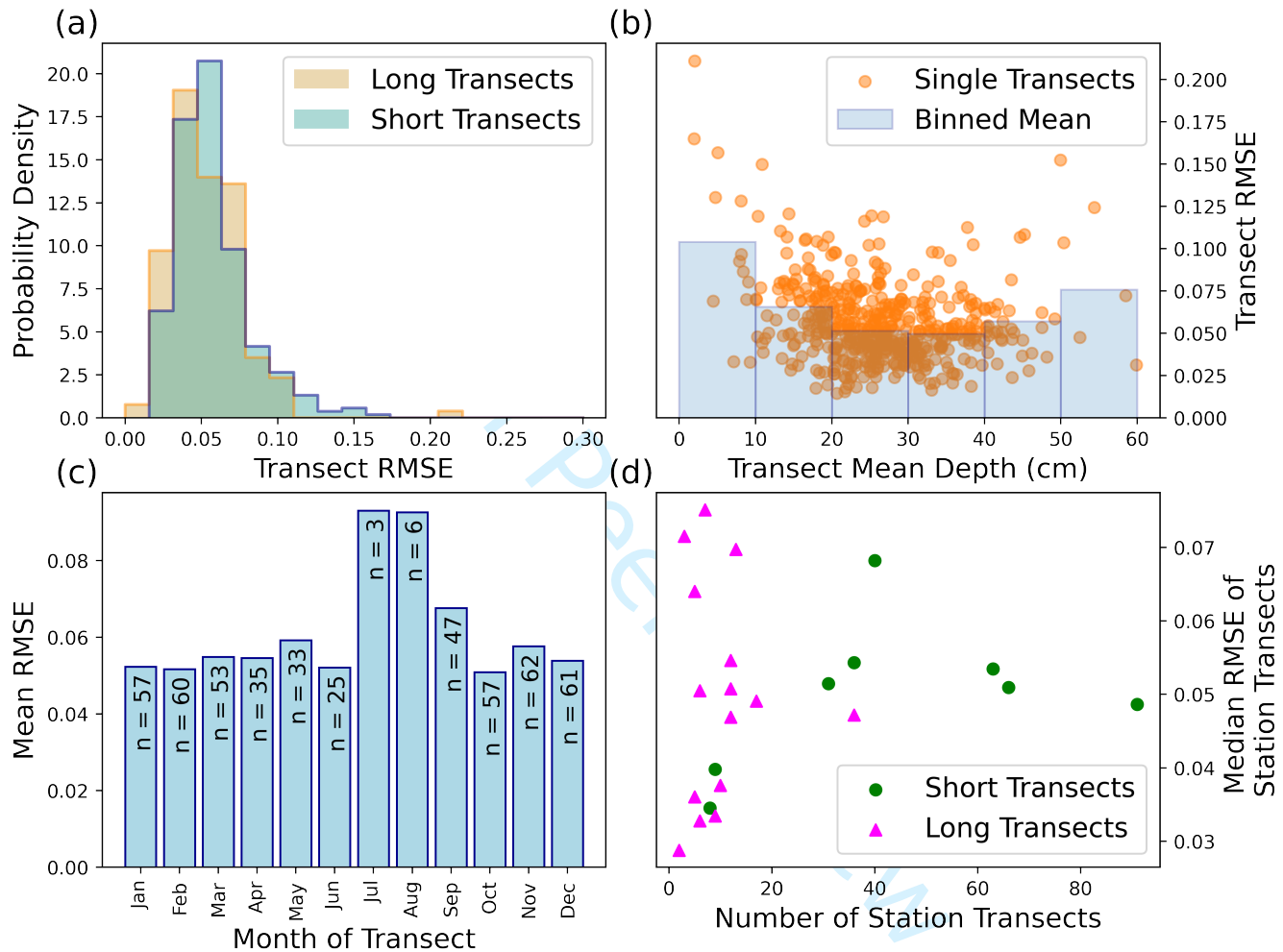


Fig. 3. (a) Histograms of the RMSE for long transects (1km) and short transects (500m) separately. (b) RMSE of the NP distribution against observed transects shown as a function of transect mean depth. (c) NP distribution RMSE as a function of month. ‘n’ indicates the number of transects contributing to the model from that month (d) Mean RMSE of all transects at a given station, shown as a function of the number of transects at that station. RMSE values are unitless as they represent the error in a probability distribution.

148 skill had very shallow depths (<10 cm). In this category the model's skill is halved relative to the 20 - 40
149 cm range. This mean-depth dependent skill reflects the relative representation of transects that contribute
150 to the NP model: the model performs best when predicting transects similar to those on which it was
151 'trained' (Fig. 2a).

152 The model's skill is relatively insensitive to the month of the year with the exception of July and August
153 (Fig. 3c). In these two summer months its skill is diminished with the RMSE being on average 67% higher
154 in these two months by comparison to the average of the other months. Again, this is ostensibly a reflection
155 of the low contributions of these months to the total number of transects: July and August contribute three
156 and six transects to the NP model respectively, whereas the other months on average each contribute 49
157 transects. Low skill in these months is also likely a reflection of the snow depths being lowest, which is also
158 associated with low skill (see Fig. 3b). We also point out that in summer a bias is introduced in the form
159 of a 'surface scattering layer' (e.g. Polashenski and others, 2012), which forms at the snow-ice interface and
160 can be penetrated by a probe despite being formed of ice rather than snow.

161 We finally address the potential lack of independence between successive transects at the same station.
162 Our LOOCV approach assumes that by not training the model with the transect being validated against, the
163 validation transect is independent. But the potential exists that information about the validation transect
164 enters the model through previous and subsequent transects at the same station that are included. If
165 successive transects are strongly related, we would expect stations that contribute more transects to the
166 model to have their transects perform better in the LOOCV exercise. We apply the non-parametric
167 Spearman's Rank test for correlation and find no statistically significant ($p < 5\%$) between the number
168 of transects contributed by a station to the model and the mean or median RMSE of its transects in the
169 LOOCV exercise (Fig. 3d). This supports the premise that LOOCV is an appropriate tool with which to
170 evaluate the skill of the NP model.

171 **Evaluation against MOSAiC Measurements**

172 We compare our regression and fitted curve (Fig. 2a, b) against the snow surveys taken on the MOSAiC
173 expedition using a magnaprobe (Figs 4, 5). To do this we select snow surveys of the "Northern Transect"
174 (Stroeve and others, 2020a), which predominantly consisted of second-year ice.

175 We first note that the NP-based regression of snow depth-standard-deviation against mean depth results
176 in an underestimation of the standard deviation of snow depths from MOSAiC (Fig. 4a). The effect of this

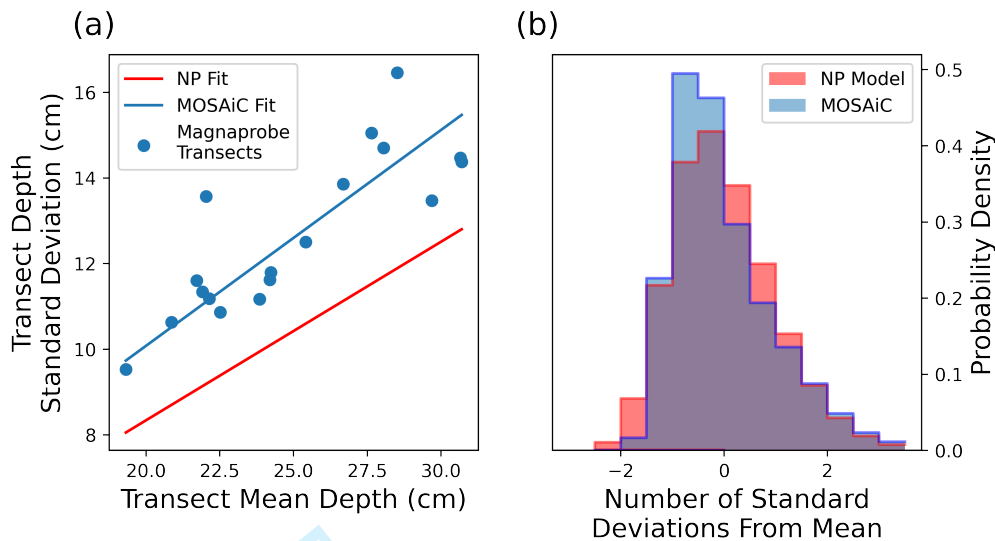


Fig. 4. (a) Snow depth variability for a given mean depth was larger on the MOSAiC transects than on average for the NP stations. Regression for NP station data shown in red, MOSAiC transects in blue. (b) Because the depth variability is lower in the NP model, the probability distribution in standard deviation space is wider (as the standard deviations themselves are smaller).

177 is that the width of the modelled depth distribution is too high in standard-deviation space (Fig. 4b). This
 178 can be understood because if the size of a standard deviation is smaller, then individual measurements end
 179 up being a higher number of smaller standard deviations away from the transect mean.

180 Despite this bias, the NP model generally provides a good fit to the individual MOSAiC transects
 181 (Fig. 5). We find that the skewness parameter of the NP model ($a = 2.54$) is smaller than when a skew-
 182 normal fit is applied to the MOSAiC transects ($a = 6.4$). This results in the modal depth bin often being
 183 overestimated by the NP model (Fig. 5). A corollary to this underestimation of skewness by the NP model
 184 is that where the modal bin is overestimated by the model, the probability (or fractional coverage) of
 185 the depth bin is underestimated. This can be seen (for example) in the panel of Fig. 5 corresponding to
 186 January 30th. The skewness parameter of data in this panel is 13.7, higher than that of the NP model. This
 187 results in the model's modal depth bin being one too high (20 - 25 cm vs 15 - 20 cm), and the probability
 188 of the modal bin being 3.5% too low.

189 The fractional coverage of shallow snow is a key parameter for light and heat flux modelling, so is now
 190 given specific consideration. We find the NP model underestimates the coverage of thin snow (<10 cm)
 191 in early winter (end of October - mid December) with respect to MOSAiC observations. The observed
 192 coverage is 6.1%, and the NP model produces a coverage of 4.3%. After mid December the model begins

Mallett and others:

11

193 to overestimate the thin snow coverage. On average it was observed to be 1.5%, and modelled to be 2.1%,
194 an overestimate by 0.6 percentage points.

For Peer Review

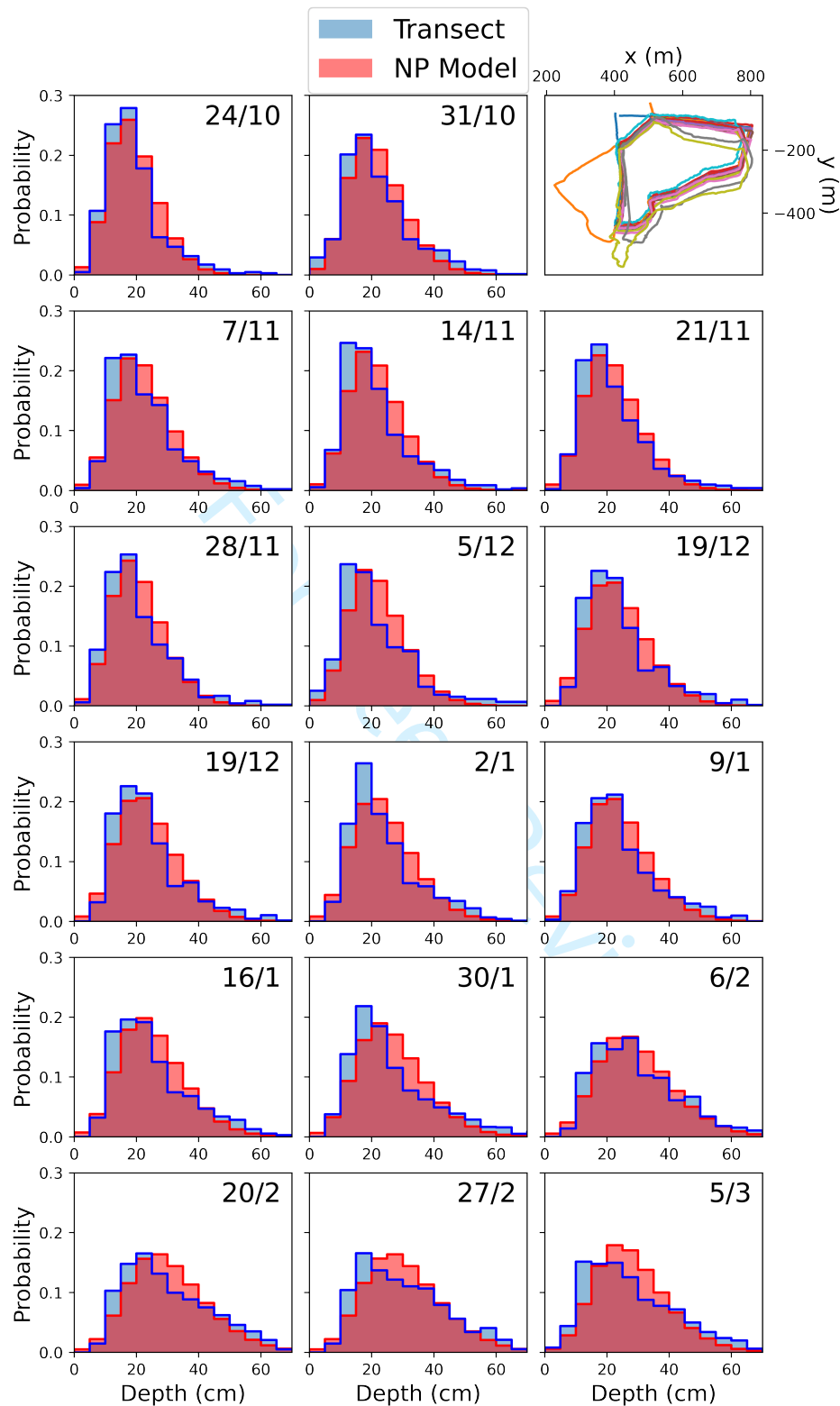


Fig. 5. Winter evolution of the snow depth distribution on the MOSAiC Northern Transect (blue histograms, 5 cm bins). The modelled depth distribution described in this paper shown in red. Top right: plots of the fourteen transects contributing to the MOSAiC evaluation exercise.

195 Evaluation against SHEBA Measurements

196 We now evaluate our method using snow depth transect data from the Surface Heat Budget of the Arctic
197 (SHEBA) expedition (Sturm and others, 2002). Snow transects were taken over a variety of ice types
198 during the SHEBA expedition, and here we opt to compare our method to transects taken in the ‘Atlanta’
199 and ‘Tuk’ areas which were dominated by multi-year ice. These areas were described using ice-class codes,
200 and were indicated as 2-3 and 4 respectively. Class 2 indicates ‘Refrozen melt ponds’, 3 ‘Hummocky’, and 4
201 ‘Deformed’ (Sturm and others, 2002). Snow depths were initially measured with a marked ski-pole, with a
202 prototype magnaprobe being used later. While the NP-model provides a good fit to the Atlanta transects,
203 it is less appropriate for Tuk transects (where the RMSE is on average doubled compared to Atlanta).

204 *Atlanta Transects*

205 We find the ratio between the transect standard deviation and the transect mean to be very similar between
206 the SHEBA and NP transects (Fig. 6a). Removing transects from the high-melting month of July from
207 the SHEBA data marginally improves this agreement, but not greatly relative to the uncertainty in the
208 regressions. We note that no transects were taken in the Atlanta region in August.

209 Unlike the standard deviation to mean depth ratio, the agreement of the snow depth distribution is
210 clearly improved by removing July transects from the SHEBA distribution (Fig. 6b). We attribute this to
211 strong alteration of the snow depth distribution by melt ponds in this month, which developed at the site
212 in the second half of June (Webster and others, 2015). Outside of this period the snow depth distribution
213 is primarily dictated by wind redistribution, but within the period it is dictated by small-scale snow surface
214 topography and resulting melt pond distribution.

215 The poor performance of our model in July and its association with intense snow melting is shown in
216 Fig. (6c). After strong melting (decreasing snow depth) in June, the snow depth distribution begins to
217 diverge from the NP model during the transition from June to July, and increases throughout July.

218 *Tuk Transects*

219 The NP model performs considerably less well when applied to Tuk transects (Fig. 7). Unlike Atlanta, the
220 standard deviation of snow depth on Tuk transects is significantly underestimated by the NP regression.
221 Furthermore, the skew-parameter of the NP model ($a = 2.54$) is less than half that of a skew-normal curve
222 fitted to the Tuk transects ($a = 6.27$).

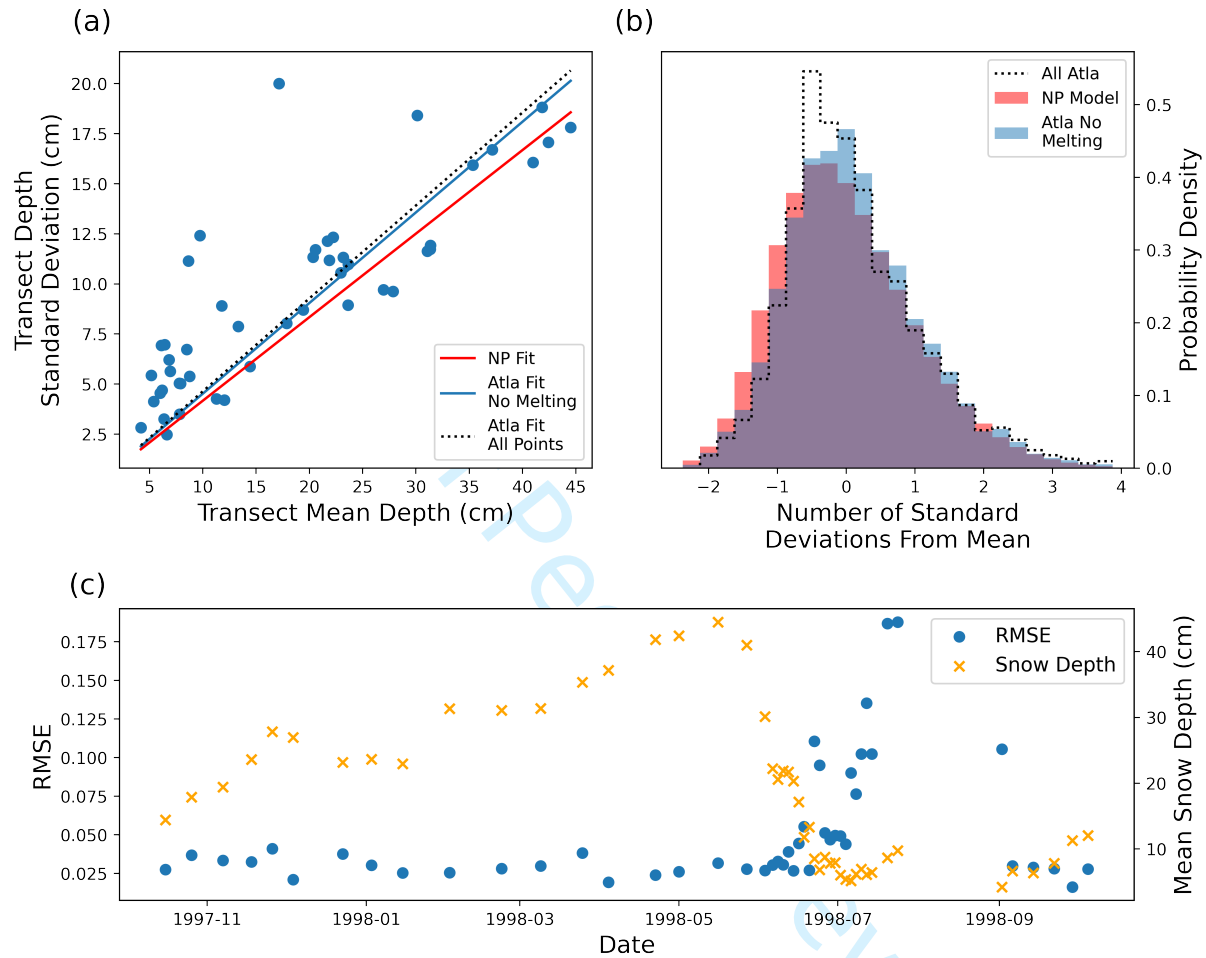


Fig. 6. (a) Relationship between the mean snow depth and standard deviation of the snow depth on SHEBA ‘Atlanta’ transects (blue scatter). Linear regressions through the points are shown both including and excluding datapoints from July and August (blue solid and black dotted lines respectively). Linear regression from all NP transects shown by red line. (b) The snow depth distribution on the SHEBA ‘Atlanta’ transect excluding July and August (blue) and from NP stations (red). The SHEBA fit from all transects including July and August shown by black dotted line. (c) Time evolution of the error in this paper’s method (blue scatter). RMSE is higher during July and August than in other months, which coincides with melted snow (depth in orange scatter).

223 It is striking that the mismatch in the skewness parameter for the Tuk transects is slightly smaller than
224 the MOSAiC transects, but the model-observations mismatch is much larger. Furthermore it is notable
225 that although the skewness of the Tuk transects is larger than the NP model, the NP model still does a
226 good job of predicting the modal depth bin. We would expect the modal bin to be too deep where the
227 skewness is underestimated (see Fig. 5). These features are explained by the fact that a skew-normal curve
228 cannot be easily fitted to the Tuk transects in standard deviation space (Fig. 8).

229 To illustrate, we display the transect data alongside the best possible skew-normal fit (not involving
230 the NP data) to the data. The agreement is good for the Atlanta and MOSAiC data sets, but noticeably
231 less good for the Tuk data (Fig. 8). This indicates that unlike the MOSAiC northern transects and the
232 SHEBA Atlanta transects, the SHEBA Tuk transects do not display a skew-normal distribution of snow
233 depths.

234 We attribute the deviation of the Tuk data from the skew-normal distribution to the highly deformed
235 nature of the ice relative to that seen at Atlanta and the MOSAiC northern transects, and at most of the
236 NP stations. Firstly we point out that over strongly deformed ice the wind dynamics may cause snow to
237 be distributed differently. Secondly we raise the fact that NP transects deviated around highly deformed
238 ice such as that dominating the Tuk transects. There is a related sampling bias for the MOSAiC Northern
239 transect, because the transect layout was chosen such that a snowmobile could drive around it.

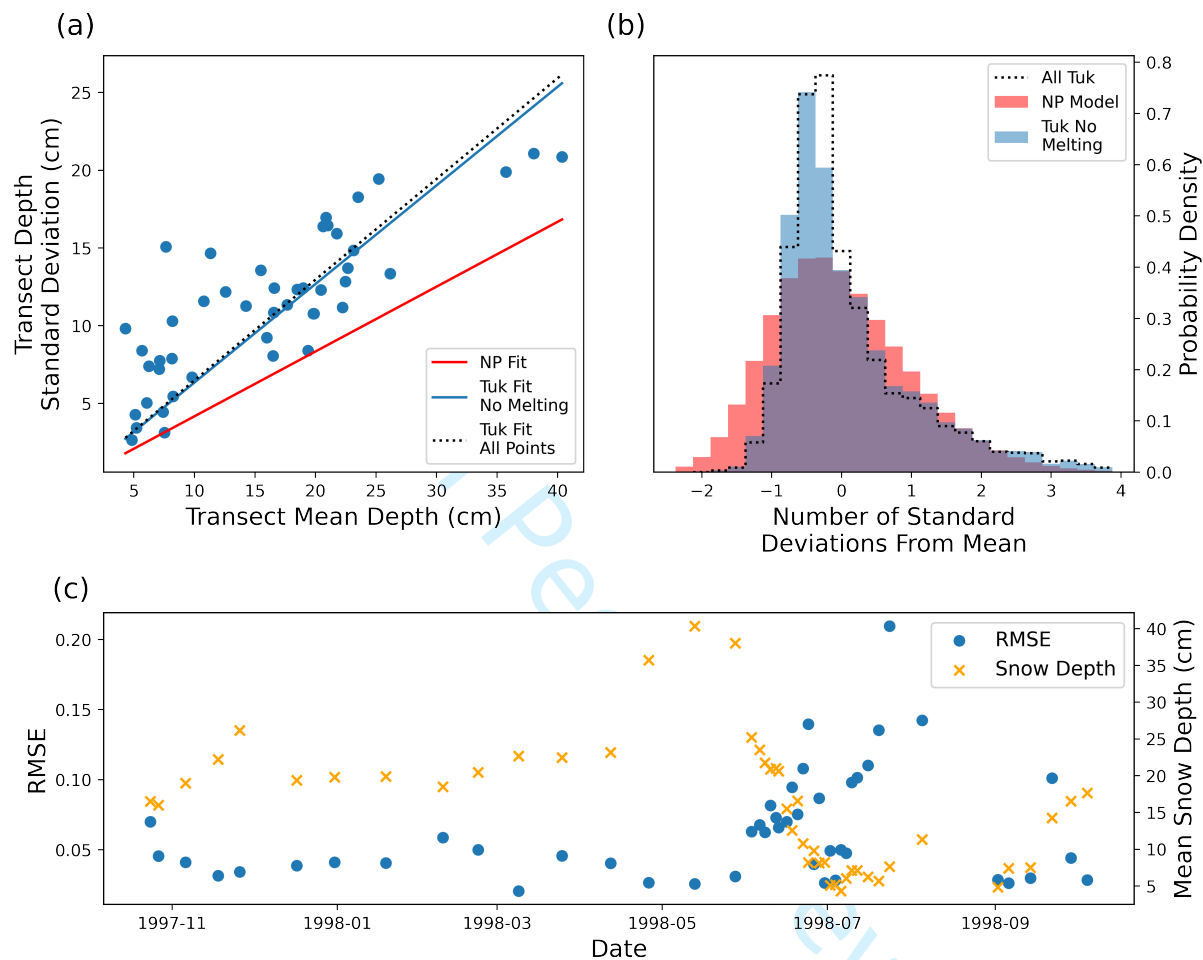


Fig. 7. (a) Relationship between the mean snow depth and standard deviation of the snow depth on SHEBA ‘Tuk’ transects (blue scatter). Linear regressions through the points are shown both including and excluding datapoints from July and August (blue solid and black dotted lines respectively). Linear regression from all NP transects shown by red line. (b) The snow depth distribution on the SHEBA ‘Tuk’ transect excluding July and August (blue) and from NP stations (red). The SHEBA fit from all transects including July and August shown by black dotted line. (c) Time evolution of the error in this paper’s method (blue scatter). RMSE is significantly higher during July and August than in other months, which coincides with melted snow (depth in orange scatter).

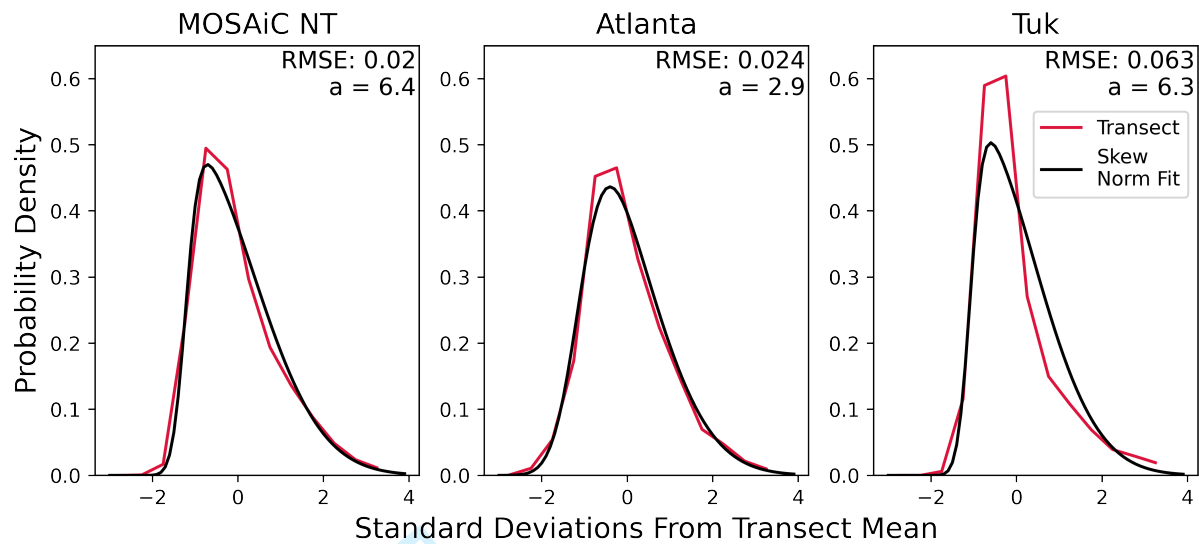


Fig. 8. Distribution of relative depth anomalies for the three evaluation data sets used in this paper (red). Distributions were generated with a bin width of 0.5 standard deviations. Skew-normal distributions are fitted to each and show variable agreement (black).

240 **Potential for Application to First Year Ice**

241 No multi-station data similar to the NP transects exist for first year ice (FYI). This is in part because first
 242 year ice cannot be drifted on for long before experiencing a melt season, but also because FYI is thinner
 243 and more liable to break up, making crewed research installations difficult to establish. Because of these
 244 difficulties, it is natural to wonder whether the NP snow depth distribution can be applied to FYI and with
 245 what uncertainty. To investigate this we apply the NP model to FYI snow depth transects taken on the
 246 AMSR-Ice03, AMSR-Ice06 (Sturm and others, 2006) and MOSAiC field campaigns (Krumpen and others,
 247 2020). Several of these transects were performed in Elson Lagoon (EL in Fig. 9), which consists of level ice.
 248 This contrasts with the more deformed ice on the nearby Beaufort sea measured during AMSR-Ice03 (BS
 249 in Fig. 9). During AMSR-Ice06 a smooth-ice section in the Chukchi Sea was also surveyed (CS in Fig. 9).
 250 Finally, during the MOSAiC expedition, successive transects were taken on a refrozen lead (nicknamed the
 251 ‘runway’, described in Stroeve and others (2020b)), which provides some information about the thin-snow
 252 regime on FYI (Fig. 9 g, h & i). For the eight transects described above we calculate the RMSE of the NP
 253 model when applied based on the mean value, calculated with 5 cm bins. We also fit a skew-normal curve
 254 to the transect data and investigate the skewness-parameter (a) to shed light on the mismatch between
 255 the NP model and the observations.

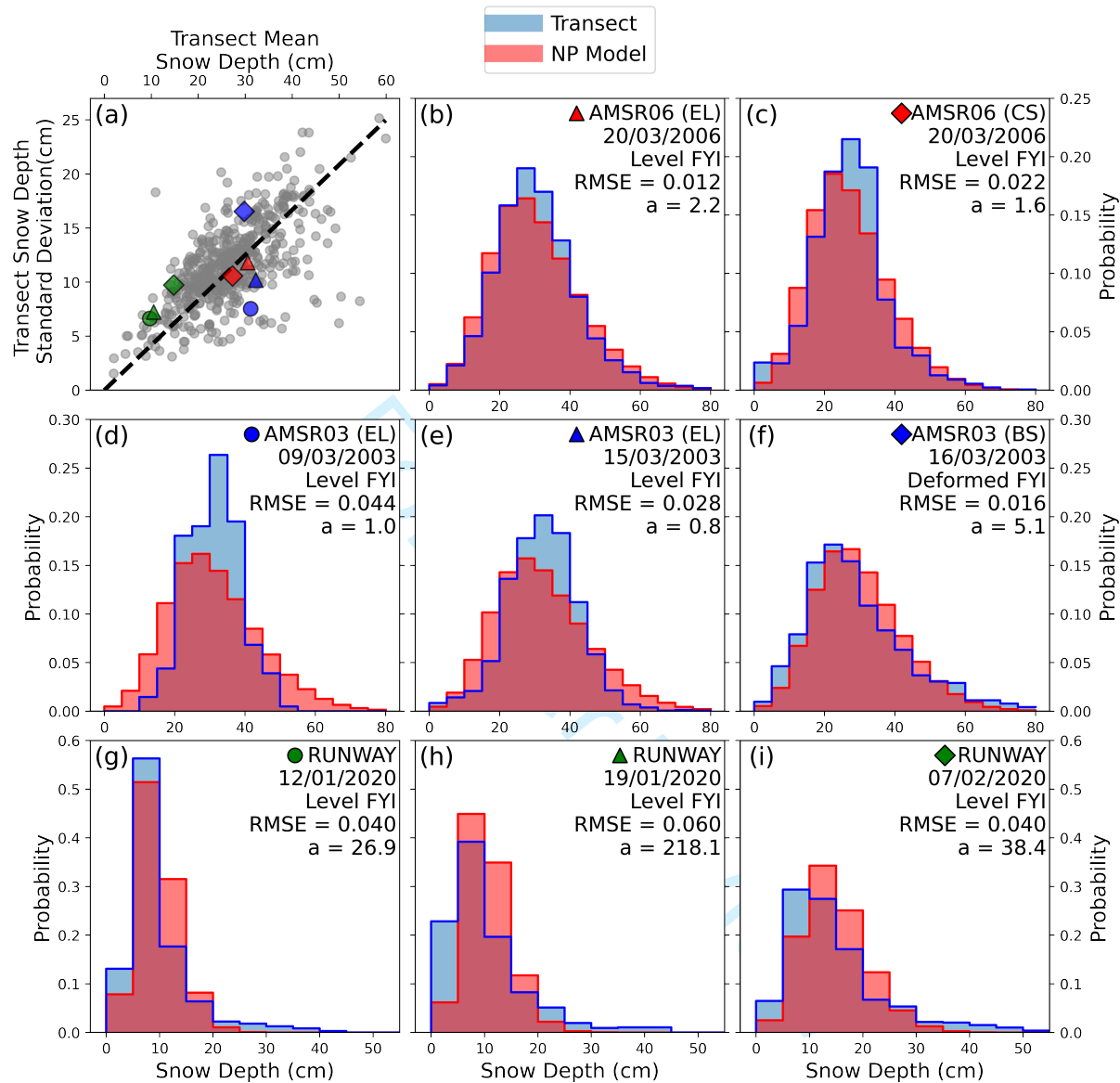


Fig. 9. Comparison of the NP model with data from first year ice transects taken during the AMSR-Ice 03, AMSR-Ice 06, and MOSAiC field campaigns. Panel (a) shows ratio of snow depth-standard-deviation to transect mean depths for the FYI transects (large markers) as well as for the NP transects (gray dots). All other panels show the snow depth distribution produced by the NP model (red) against the transects (blue), with 5 cm wide depth bins for comparative purposes. Panels represent (in order b-i) Elson Lagoon (EL) and level ice on the Chukchi Sea (b & c), two transects on Elson Lagoon one week apart (d & e), a transect on FYI of the Beaufort sea near Elson Lagoon (f). Bottom row (g - i) displays snow transects taken on a refrozen lead during the MOSAiC expedition.

256 We first observe that all eight FYI transects have ratios of depth-standard-deviation to mean depth
257 roughly consistent with that observed in the NP stations (Fig. 9a), particularly those from AMSR-Ice06.
258 We also note that the skewness parameter of the AMSR-Ice06 data ($a = 1.6$ & 2.2) is close to the skewness
259 parameter of the NP-model ($a = 2.54$). These characteristics lead to the NP model performing better
260 on the AMSR-Ice06 data than the AMSR-Ice03 data. The AMSR-Ice06 survey on Elson Lagoon has the
261 lowest RMSE of all eight FYI transects (0.012) when compared to the NP model - this is related to it
262 having the most closely matching skewness parameter to the NP model.

263 While all three AMSR-Ice03 transects have very similar mean snow depths to each other (~ 30 cm),
264 we find that the ratio of depth-standard-deviation to mean snow depth is lower than for the NP station
265 transects for the Elson Lagoon transects, but higher for the Beaufort Sea (Fig. 9a). That is to say, the
266 snow over the deformed first year ice in the Beaufort Sea exhibited considerably more variability than that
267 over the smooth ice in Elson Lagoon during AMSR-Ice03. In addition to being more variable, the Beaufort
268 Sea transect showed a much higher skewness parameter ($a = 5.14$) than those on Elson Lagoon ($a = 1.02$
269 & 0.844). Because a skewness parameter of 1 represents a symmetrical distribution, it follows that the
270 transect on the 15th March on Elson Lagoon was skewed the *other* way to that typical of the other surveys
271 studied in this paper. The transect over deformed ice exhibits the lowest RMSE value of the AMSR-Ice03
272 transects by some margin.

273 We attribute the low-skewness (symmetry) of the 2003 Elson Lagoon data to a lack of ice topography
274 around which to build up a 'long tail' of drifted, thick snow. Conversely, the highly deformed ice of the
275 Beaufort Sea produces a noticeable long tail of thick snow, such that the probability of finding snow deeper
276 than 55 cm is underestimated by the NP model (Fig. 9f). However it is striking that the AMSR-Ice06
277 transects at Elson Lagoon are more weakly governed by this: while the skewness parameters are still lower
278 than for the NP transects, there is a smaller difference.

279 We now turn to the thin snow cover of the three MOSAiC 'runway' transects (Fig. 9 g, h & i). We
280 first point out that a skew-normal curve cannot be easily fitted to these data (not shown; similar to the
281 situation with the SHEBA 'Tuk' transects above). This indicates that the NP model will not be a good
282 fit, even before it is applied. Because of this feature, the skewness-parameter values listed in the panels
283 of Fig. 9 should not be understood to properly capture the underlying transect data. When the NP
284 model is applied and compared, it exhibits a high RMSE relative to the other FYI transects. As well as
285 being related to the poor approximation with a skew-normal curve, this performance is also linked to the

three ‘runway’ transects having the highest error in depth-standard-deviation to mean depth ratio (Fig. 9a) by comparison to the NP transects. One key physical difference between the runway transects and the other FYI surveys is the low average snow depth. However other contextual differences exist: for example the transects were performed in a colder region (near the pole), and at a colder time of year (January/February). This may result in a more weakly bonded snowpack at the time of measurement, susceptible to more wind-redistribution and resulting in a higher depth-standard-deviation to mean-depth ratio (by comparison to the AMSR-Ice transects).

Because of the differences in the age of the snow (and the ice topography over level ice), there is no a priori reason that the NP-model for the snow depth distribution derived in this paper should be applicable to FYI, and indeed our model works relatively poorly when simulating the ‘symmetrical’ snow depth distributions at Elson Lagoon in 2003, and the thin snow on the MOSAiC runway.

However in the instance where the ice was deformed (Fig. 9f) the model performs relatively well. Perhaps counterintuitively given the 2003 results, the NP model also performed well in 2006 over both level ice transects. The RMSE of the NP Model when applied to the Beaufort Sea transect was 0.016, which is in fact lower than the corresponding values for the MOSAiC Northern Transects (Fig. 5), which ranged from 0.019 - 0.031. By this metric the performance of the model over FYI in 2006 was also better (0.012) and comparable (0.022).

In summary, we have shown that the NP model is capable of performing well over deformed FYI, and even over level ice in the case of 2006 (where ‘well’ is defined with reference to its performance over MYI at MOSAiC). But despite this capability, it also clearly performs poorly in the case of thin snow (MOSAiC runway, where we observed that the measurements could not be well-represented by any skew-normal distribution), and also in the case of highly symmetrical (low-skew) snow distributions over FYI (Elson Lagoon in 2003).

Application to point-measurements of snow depth

There are several drifting, autonomous platforms in existence that record the snow depth at a single point, such as snow buoys and ice mass balance buoys (Nicolaus and others, 2021). If the buoy is deployed at random, it is most likely to sample the modal snow depth. In reality these instruments are often not deployed at random, and a conscious choice is made to sample what is perceived to be the modal depth. However for applications such as laser and radar altimetry retrievals of sea ice thickness, the mean snow

315 depth is the quantity required for characterising the floe's hydrostatic equilibrium (e.g. Mallett and others,
 316 2021). We now present a simple method of relating these point measurements to the mean snow depth of
 317 the surrounding area.

318 If the mean snow depth (\bar{D}) is related linearly to the standard deviation (σ_D , Fig. 2a, Eq. 1) by a
 319 constant K , and we observe the modal snow depth to be X standard deviations below the mean (Fig. 2b),
 320 then we can relate the modal depth to the mean depth as follows:

$$\sigma_D = K\bar{D} \quad \& \quad \bar{D} = D_{mode} + X\sigma_D \quad (4)$$

$$\bar{D} = \frac{D_{mode}}{(1 - XK)} \quad (5)$$

321 Using the NP data from Fig. (2) we now calculate that $X = 0.35$. The value of K was found earlier
 322 (Eq. 1) to be 0.417. We therefore calculate that the mean snow depth is 17% larger than the modal depth.
 323 Where singular drifting instruments are assumed to retrieve the modal snow depth in their environment,
 324 we recommend this correction for estimation of the mean.

325 Length Scales

326 The NP station transects were performed over distances of 500 - 1000 m, and this characterises the length
 327 scale on which our distribution is relevant. If the same transects were theoretically performed over just
 328 a few centimetres, the ratio of the standard deviation in snow depth to the mean snow depth (Fig. 2a)
 329 would be lower, and the distribution about the mean would likely be different. The distribution would be
 330 sensitive to the small-scale roughness of the snow surface, rather than larger scale features like sastrugi and
 331 snow drifts around ice topography. If the transects were performed (again, theoretically) over thousands
 332 of kilometres then the snow distribution would again be different, and more representative of synoptic
 333 variability in snowfall and ice type. As such we stress that we have characterised the distribution of snow
 334 depth at the *sub-kilometre* length scale (on the order of hundreds of metres).

335 We also conduct an analysis to ensure that our results are robust to the spatial sampling interval of the
 336 transects, which was 10 m for the NP stations. We investigate whether Fig. 2 and the resulting NP model
 337 would be different if the transects had five or ten times the spacing. We find that artificially increasing
 338 the spacing of measurements by only considering one in every five or ten measurements (sampling at 50

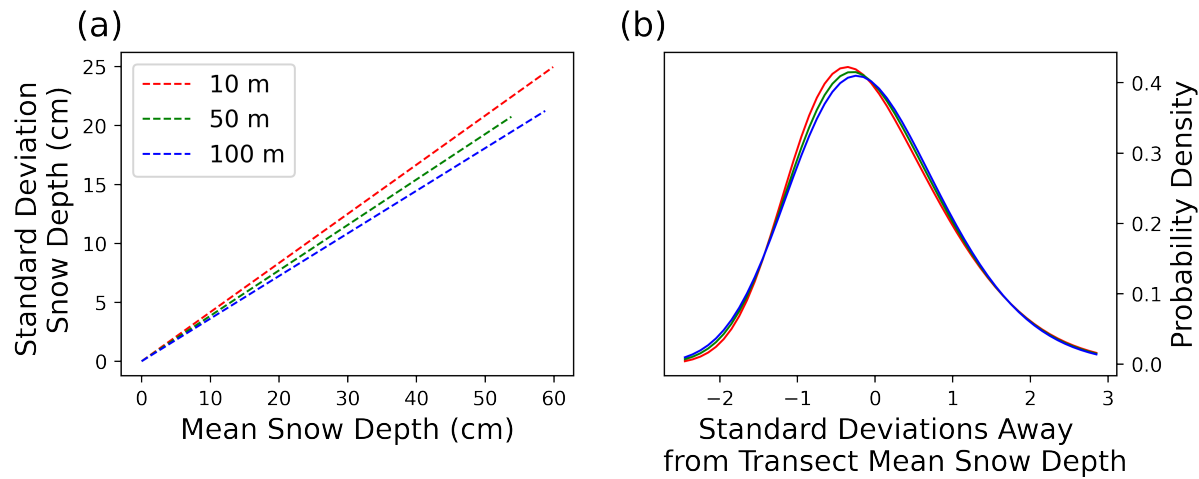


Fig. 10. Impact of undersampling the transect by taking every fifth and tenth measurement on (a) the ratio of transect standard deviation to transect mean snow depth (b) the probability density distribution in standard deviation space.

339 and 100 m respectively) has a small impact on the ratio of the standard deviation to the mean, and the
 340 parameters of the skew-normal curve of best fit (Fig. 10). When comparing a 10 m sampling interval to
 341 a 100 m sampling interval, the standard deviation to mean depth ratio decreases from 0.416 to 0.361, and
 342 the skewness parameter to decrease from 2.54 to 1.84. Extrapolating from this trend, magnaprobe samples
 343 used in the validation data sets which have a sampling interval of 1 m may therefore have a high-skew
 344 and high $\sigma_D : \bar{D}$ bias relative to transects from NP stations.

345 **Relevance in a changing Arctic Ocean and other limitations**

346 The potential for application of the NP-model to first year ice was discussed above, and it was found that
 347 while the NP model was capable of performing well over FYI, it performed poorly when simulating the
 348 distribution of thin snow, and overestimated the skew in some cases. Here we point out that the Arctic
 349 Ocean is becoming increasingly dominated by first year ice, so arguably the relevance of this MYI-trained
 350 model is in slow decline.

351 There may also be spatial limitations on applicability. The NP drifting stations generally operated
 352 in the Central Arctic Ocean rather than in the marginal regions such as the Kara, Beaufort and Barents
 353 Seas (Warren and others, 1999). However these areas are generally dominated by first year ice, so this
 354 geographic constraint is less strict than the ice-type one described above.

355 The average age of multi-year ice is in decline, with the coverage of ice aged five years or more shrinking

356 from 28% to 1.9% between 1984 and 2018 (Stroeve and Notz, 2018). The mean thickness of sea ice is also
357 in decline (Kwok, 2018). Because we produce our statistical model using drifting station data from 1955 -
358 1991, it likely reflects snow conditions on ice older and thicker than that which currently exists in the Arctic.
359 We note however that our method does still display good skill with respect to the MOSAiC transects, which
360 were generally performed on ice that had only experienced one melt season.

361 SUMMARY

362 In this paper we have developed a generic snow depth distribution for multi-year ice that can be fully
363 characterised by the mean snow depth. This allows it to be superimposed onto estimates of mean snow
364 depth from satellites and models for the purposes of flux modelling and altimetry studies.

365 We performed a cross-validation exercise and found the model's skill to be highest in winter, and lowest
366 during the summer months of intense melt and sparse measurements. We then evaluated the distribution
367 against snow depth transects from the MOSAiC, SHEBA and AMSR-Ice field campaigns. We found that
368 the model generally overestimated the variability in snow depths for the MOSAiC campaign, but the fit
369 parameters were otherwise broadly appropriate. On the smoother multiyear ice of the SHEBA campaign
370 the model performed well, but the model performed poorly on transects executed over highly deformed
371 ice. We found that this was related to the fact that the snow depth distribution in this area was not well
372 approximated by the skewed normal distribution used in the NP model. We then applied the distribution to
373 eight transects conducted over first year ice, and found that while the NP-model was capable of performing
374 well (over deformed FYI and in two cases over level ice), it performed poorly when simulating thin snow
375 on a refrozen lead in the Central Arctic, and also when simulating a highly symmetrical snow distribution
376 over level ice.

377 Acknowledgements

378 This work was funded primarily by the London Natural Environment Research Council (NERC) Doctoral
379 Training Partnership (DTP) grant (NE/L002485/1). JCS acknowledges support from the Canada 150
380 Chair Program and NASA grants NNX16AJ92G, 80NSSC20K1121 & 19-ICESAT2-19-0088; ‘Sunlight
381 under sea ice’. MT acknowledges support from the European Space Agency ‘Polarice’ grant ESA/AO/1-
382 9132/17/NL/MP, NERC grant NE/S002510/1, NERC “PRE-MELT” NE/T000546/1 project and from the
383 ESA “EXPRO+ Snow” (ESA AO/1-10061/19/I-EF) project. VN was supported by JCS, in part thanks to
384 the Canada 150 Chair Program. RW was supported by NERC grant NE/S002510/1. PI acknowledges
385 funding from the Research Council of Norway (RCN287871, SIDRiFT) and the US National Science
386 Foundation (NSF) (NSF1820927, MiSNOW). MO acknowledges funding from the NSF (OPP1735862).
387 MJ acknowledges funding from the NSF (NSF1820927, MiSNOW). JL acknowledges support from the
388 Centre for Integrated Remote Sensing and Forecasting for Arctic Operations (CIRFA) project through the
389 Research Council of Norway (RCN) under Grant 237906.

390 Code and Data Availability

391 All code and data required to reproduce this analysis can be downloaded from [github/robbiemallett/sub_km](https://github.com/robbiemallett/sub_km).

392 REFERENCES

- 393 Azzalini A and Capitanio A (1999) Statistical applications of the multivariate skew normal distribution. *Journal of the*
394 *Royal Statistical Society: Series B (Statistical Methodology)*, **61**(3), 579–602, ISSN 1369-7412 (doi: 10.1111/1467-
395 9868.00194)
- 396 Chung YC, Bélair S and Mailhot J (2011) Blowing snow on arctic sea ice: Results from an improved sea
397 ice-snow-blowing snow coupled system. *Journal of Hydrometeorology*, **12**(4), 678–689, ISSN 1525755X (doi:
398 10.1175/2011JHM1293.1)
- 399 Eicken H, Lange MA and Wadhams P (1994) Characteristics and distribution patterns of snow and meteoric ice in
400 the Weddell Sea and their contribution to the mass balance of sea ice. *Annales Geophysicae*, **12**(1), 80–93, ISSN
401 14320576 (doi: 10.1007/s00585-994-0080-x)
- 402 Filhol S and Sturm M (2015) Snow bedforms: A review, new data, and a formation model. *Journal of Geophysical*
403 *Research: Earth Surface*, **120**(9), 1645–1669, ISSN 21699003 (doi: 10.1002/2015JF003529)

- 404 Glissenaar IA, Landy JC, Petty AA, Kurtz NT and Stroeve JC (2021) Impacts of snow data and processing methods
405 on the interpretation of long-term changes in Baffin Bay sea ice thickness. *The Cryosphere Discussions*, **2021**,
406 1–26 (doi: 10.5194/tc-2021-135)
- 407 Iacozza J and Barber DG (1999) An examination of the distribution of snow on sea-ice. *Atmosphere - Ocean*, **37**(1),
408 21–51, ISSN 14809214 (doi: 10.1080/07055900.1999.9649620)
- 409 Krumpfen T, Birrien F, Kauker F, Rackow T, von Albedyll L, Angelopoulos M, Belter HJ, Bessonov V, Damm E,
410 Dethloff K, Haapala J, Haas C, Harris C, Hendricks S, Hoelemann J, Hoppmann M, Kaleschke L, Karcher M,
411 Kolabutin N, Lei R, Lenz J, Morgenstern A, Nicolaus M, Nixdorf U, Petrovsky T, Rabe B, Rabenstein L, Rex M,
412 Ricker R, Rohde J, Shimanchuk E, Singha S, Smolyanitsky V, Sokolov V, Stanton T, Timofeeva A, Tsamados M
413 and Watkins D (2020) The MOSAiC ice floe: sediment-laden survivor from the Siberian shelf. *The Cryosphere*,
414 **14**(7), 2173–2187, ISSN 1994-0424 (doi: 10.5194/tc-14-2173-2020)
- 415 Kwok R (2018) Arctic sea ice thickness, volume, and multiyear ice coverage: Losses and coupled variability (1958-
416 2018). *Environmental Research Letters*, **13**(10), 105005, ISSN 17489326 (doi: 10.1088/1748-9326/aae3ec)
- 417 Lawrence IR, Tsamados MC, Stroeve JC, Armitage TW and Ridout AL (2018) Estimating snow depth over Arctic
418 sea ice from calibrated dual-frequency radar freeboards. *Cryosphere*, **12**(11), 3551–3564, ISSN 19940424 (doi:
419 10.5194/tc-12-3551-2018)
- 420 Liston GE, Polashenski C, Rösel A, Itkin P, King J, Merkouriadi I and Haapala J (2018) A Distributed Snow-Evolution
421 Model for Sea-Ice Applications (SnowModel). *Journal of Geophysical Research: Oceans*, **123**(5), 3786–3810, ISSN
422 21699291 (doi: 10.1002/2017JC013706)
- 423 Liston GE, Itkin P, Stroeve J, Tschudi M, Stewart JS, Pedersen SH, Reinking AK and Elder K (2020) A Lagrangian
424 Snow-Evolution System for Sea-Ice Applications (SnowModel-LG): Part I – Model Description. *Journal of*
425 *Geophysical Research: Oceans*, **125**(10), e2019JC015913, ISSN 2169-9275 (doi: 10.1029/2019jc015913)
- 426 Mallett RDC, Stroeve JC, Tsamados M, Landy JC, Willatt R, Nandan V and Liston GE (2021) Faster decline and
427 higher variability in the sea ice thickness of the marginal Arctic seas when accounting for dynamic snow cover.
428 *The Cryosphere*, **15**(5), 2429–2450, ISSN 1994-0424 (doi: 10.5194/tc-15-2429-2021)
- 429 Massom RA, Drinkwater MR and Haas C (1997) Winter snow cover on sea ice in the Weddell Sea. *Journal of*
430 *Geophysical Research: Oceans*, **102**(C1), 1101–1117, ISSN 01480227 (doi: 10.1029/96JC02992)
- 431 Moon W, Nandan V, Scharien RK, Wilkinson J, Yackel JJ, Barrett A, Lawrence I, Segal RA, Stroeve J, Mahmud
432 M, Duke PJ and Else B (2019) Physical length scales of wind-blown snow redistribution and accumulation on
433 relatively smooth Arctic first-year sea ice. *Environmental Research Letters*, **14**(10), 104003, ISSN 1748-9326 (doi:
434 10.1088/1748-9326/ab3b8d)

- 435 Nicolaus M, Hoppmann M, Arndt S, Hendricks S, Katlein C, Nicolaus A, Rossmann L, Schiller M and Schwegmann S
436 (2021) Snow Depth and Air Temperature Seasonality on Sea Ice Derived From Snow Buoy Measurements. *Frontiers*
437 *in Marine Science*, **8**, 377, ISSN 2296-7745 (doi: 10.3389/fmars.2021.655446)
- 438 O'Hagan A and Leonard T (1976) Bayes estimation subject to uncertainty about parameter constraints. *Biometrika*,
439 **63**(1), 201–203, ISSN 0006-3444 (doi: 10.1093/biomet/63.1.201)
- 440 Petty AA, Webster M, Boisvert L and Markus T (2018) The NASA Eulerian Snow on Sea Ice Model (NESOSIM)
441 v1.0: Initial model development and analysis. *Geoscientific Model Development*, **11**(11), 4577–4602, ISSN 19919603
442 (doi: 10.5194/gmd-11-4577-2018)
- 443 Petty AA, Kurtz NT, Kwok R, Markus T and Neumann TA (2020) Winter Arctic Sea Ice Thickness From ICESat-2
444 Freeboards. *Journal of Geophysical Research: Oceans*, **125**(5), ISSN 21699291 (doi: 10.1029/2019JC015764)
- 445 Polashenski C, Perovich D and Courville Z (2012) The mechanisms of sea ice melt pond formation and evolution.
446 *Journal of Geophysical Research: Oceans*, **117**(C1), 1001, ISSN 2156-2202 (doi: 10.1029/2011JC007231)
- 447 Rostosky P, Spreen G, Farrell SL, Frost T, Heygster G and Melsheimer C (2018) Snow Depth Retrieval on
448 Arctic Sea Ice From Passive Microwave Radiometers—Improvements and Extensions to Multiyear Ice Using
449 Lower Frequencies. *Journal of Geophysical Research: Oceans*, **123**(10), 7120–7138, ISSN 21699291 (doi:
450 10.1029/2018JC014028)
- 451 Stone M (1978) Cross-validation: a review. *Series Statistics*, **9**(1), 127–139, ISSN 0323-3944 (doi:
452 10.1080/02331887808801414)
- 453 Stroeve J and Notz D (2018) Changing state of Arctic sea ice across all seasons. *Environmental Research Letters*,
454 **13**(10), 103001, ISSN 17489326 (doi: 10.1088/1748-9326/aade56)
- 455 Stroeve J, Liston GE, Buzzard S, Zhou L, Mallett R, Barrett A, Tschudi M, Tsamados M, Itkin P and Stewart
456 JS (2020a) A Lagrangian Snow-Evolution System for Sea Ice Applications (SnowModel-LG): Part II - Analyses.
457 *Journal of Geophysical Research: Oceans*, **125**(10), e2019JC015900, ISSN 2169-9275 (doi: 10.1029/2019JC015900)
- 458 Stroeve J, Nandan V, Willatt R, Tonboe R, Hendricks S, Ricker R, Mead J, Mallett R, Huntemann M, Itkin P,
459 Schneebeli M, Krampe D, Spreen G, Wilkinson J, Matero I, Hoppmann M and Tsamados M (2020b) Surface-based
460 Ku-and Ka-band polarimetric radar for sea ice studies. *Cryosphere*, **14**(12), 4405–4426 (doi: 10.5194/TC-14-4405-
461 2020)
- 462 Stroeve J, Vancoppenolle M, Veyssiere G, Lebrun M, Castellani G, Babin M, Karcher M, Landy J, Liston GE
463 and Wilkinson J (2021) A Multi-Sensor and Modeling Approach for Mapping Light Under Sea Ice During the
464 Ice-Growth Season. *Frontiers in Marine Science*, **7**, 1253, ISSN 22967745 (doi: 10.3389/fmars.2020.592337)

- 465 Sturm M, Holmgren J and Perovich DK (2002) Winter snow cover on the sea ice of the Arctic Ocean at the Surface
466 Heat Budget of the Arctic Ocean (SHEBA): Temporal evolution and spatial variability. *Journal of Geophysical*
467 *Research C: Oceans*, **107**(10), 1–17, ISSN 01480227 (doi: 10.1029/2000jc000400)
- 468 Sturm M, Maslanik JA, Perovich DK, Stroeve JC, Richter-Menge J, Markus T, Holmgren J, Heinrichs JF and
469 Tape K (2006) Snow depth and ice thickness measurements from the Beaufort and Chukchi Seas collected during
470 the AMSR-Ice03 Campaign. *IEEE Transactions on Geoscience and Remote Sensing*, **44**(11), 3009–3019, ISSN
471 01962892 (doi: 10.1109/TGRS.2006.878236)
- 472 Warren SG (2019) Optical properties of ice and snow. *Philosophical Transactions of the Royal Society A:*
473 *Mathematical, Physical and Engineering Sciences*, **377**(2146), ISSN 1364503X (doi: 10.1098/rsta.2018.0161)
- 474 Warren SG, Rigor IG, Untersteiner N, Radionov VF, Bryazgin NN, Aleksandrov YI and Colony R (1999)
475 Snow depth on Arctic sea ice. *Journal of Climate*, **12**(6), 1814–1829, ISSN 08948755 (doi: 10.1175/1520-
476 0442(1999)012<1814:SDOASI>2.0.CO;2)
- 477 Webster MA, Rigor IG, Perovich DK, Richter-Menge JA, Polashenski CM and Light B (2015) Seasonal evolution of
478 melt ponds on Arctic sea ice. *Journal of Geophysical Research: Oceans*, **120**(9), 5968–5982, ISSN 21699291 (doi:
479 10.1002/2015JC011030)
- 480 Zhou L, Stroeve J, Xu S, Petty A, Tilling R, Winstrup M, Rostosky P, Lawrence IR, Liston GE, Ridout A, Tsamados
481 M and Nandan V (2021) Inter-comparison of snow depth over Arctic sea ice from reanalysis reconstructions and
482 satellite retrieval. *Cryosphere*, **15**(1), 345–367, ISSN 19940424 (doi: 10.5194/tc-15-345-2021)